Supplementary Information (SI) for Dalton Transactions.
This journal is © The Royal Society of Chemistry 2024

Supporting Information for

Facile room temperature synthesis of layered transition metal phosphonates via hitherto unknown alkali metal tert-butyl phosphonates

Anuj Kumar, Aheli Ghatak, and Ramaswamy Murugavel*

Department of Chemistry, Indian Institute of Technology Bombay, Powai, Mumbai 400017, India, E-mail: rmv@chem.iitb.ac.in

Fig. S1 FT-IR spectra of **1-3** as KBr discs.

Fig. S2 ^{31}P NMR spectrum of **1-3**

Fig. S3 CP-MAS ^{7}Li NMR spectrum of **1** (233 MHz).

Fig. S4 CP-MAS ^{13}C NMR spectrum of **1** (150 MHz).

Fig. S5 The CP-MAS ^{13}C NMR spectrum of **2** (100 MHz).

Fig. S6 The CP-MAS ^{13}C NMR spectrum of **3** (125 MHz).

Table S1 Shape analysis in complex **1.**

Table S2 Shape analysis in complex **2.**

Table S3 Shape analysis in complex **3.**

Table S4 Selected bond distances (Å) and bond angles (º) in **1**.

Table S5 Hydrogen bonds (Å) and angles (º) for **1**.

Table S6 Selected bond distances (Å) and bond angles (º) in **2**.

Table S7 Hydrogen bonds (Å) and angles (º) for **2**.

Table S8 Selected bond distances (Å) and bond angles (º) in **3**.

Table S9 Hydrogen bonds (Å) and angles (º) for **3**.

Fig. S7 TGA profile of compounds **1**

Fig. S8 TGA profile of compounds **2**

Fig. S9 TGA profile of compounds **3**

Fig. S10 SEM images of compound **1** with elemental mapping

Fig. S11 SEM images of compound **2** with elemental mapping

Fig. S12 SEM images of compound **3** with elemental mapping

Fig. S13 PXRD pattern of **1**

Fig. S14 PXRD pattern of **2**

Fig. S15 PXRD pattern of **3**

Fig. S16 Comparison of FT-IR spectra of **4-6** with **2** as KBr diluted discs.

Fig. S17 PXRD pattern of **6**

Fig. S18 SEM images of compound **4** with elemental mapping

Fig. S19 SEM images of compound **6** with elemental mapping

Fig. S20 DR-UV of compound **4**

Fig. S21 DR-UV of compound **5**

Fig. S22 DR-UV of compound **6**

Fig. S23 TGA profile of compounds **4**

Fig. S24 TGA profile of compounds **5**

Fig. S25 TGA profile of compounds **6**

Fig. S26 CP-MAS ^{31}P NMR spectrum of **4** (162 MHz)

Fig. S27 Elemental analysis of **1**

Fig. S28 Elemental analysis of **2**

Fig. S29 Elemental analysis of **3**

Fig. S30 Elemental analysis of **4**

Fig. S31 Elemental analysis of **5**

Fig. S32 Elemental analysis of **6**

Table S10. Chemical composition of **1**-**3** measured with ICP-AES

Table S11. Chemical composition of **4**-**6** measured with ICP-AES

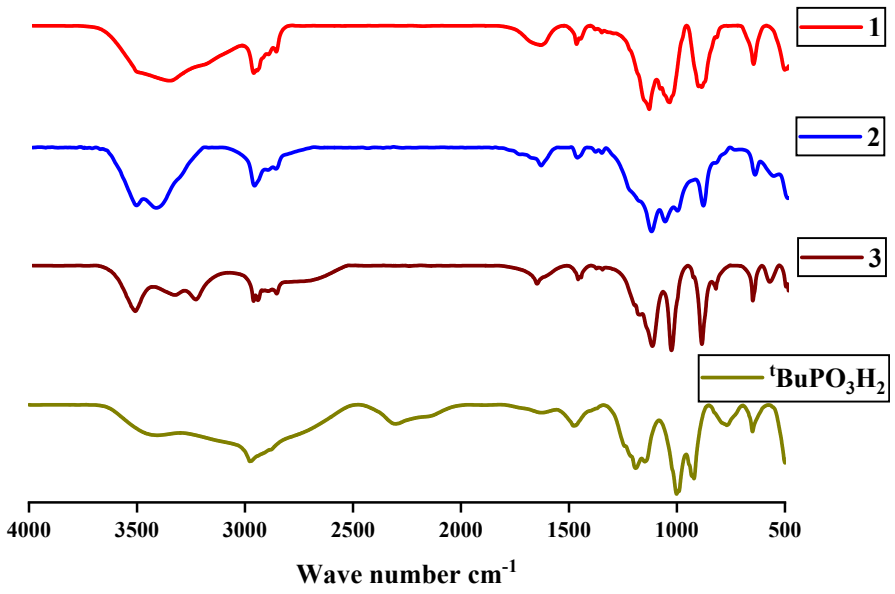

Fig. S1 FT-IR spectra of **1-3** (as KBr Discs).

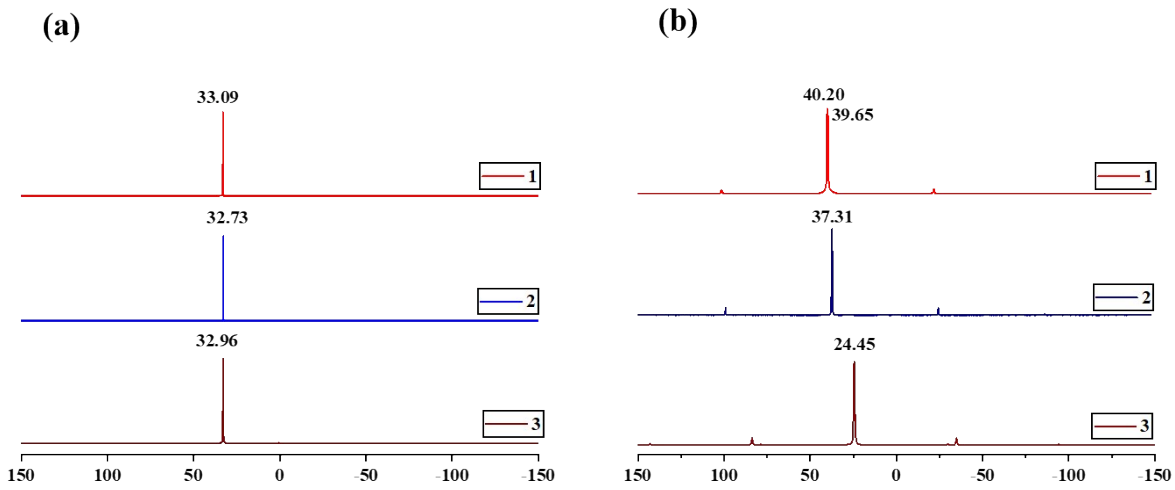

Fig. S2 (a) ^{31}P NMR spectrum of **1-3 (**in D_2O, 202 MHz Left), (b) CP-MAS ^{31}P NMR spectrum of **1** and **2** (162 MHz), and **3** (202 MHz) (δ in ppm).

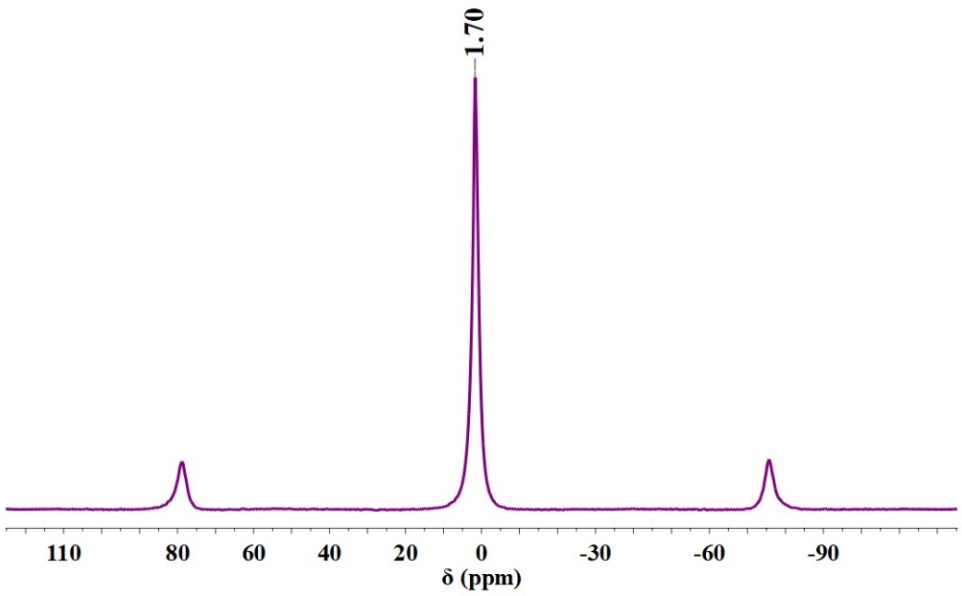

Fig. S3 CP-MAS ^{7}Li NMR spectrum of [(^{t}BuPO$_3$H)Li(H$_2$O)$_3$·(H$_2$O)] **1** (233 MHz).

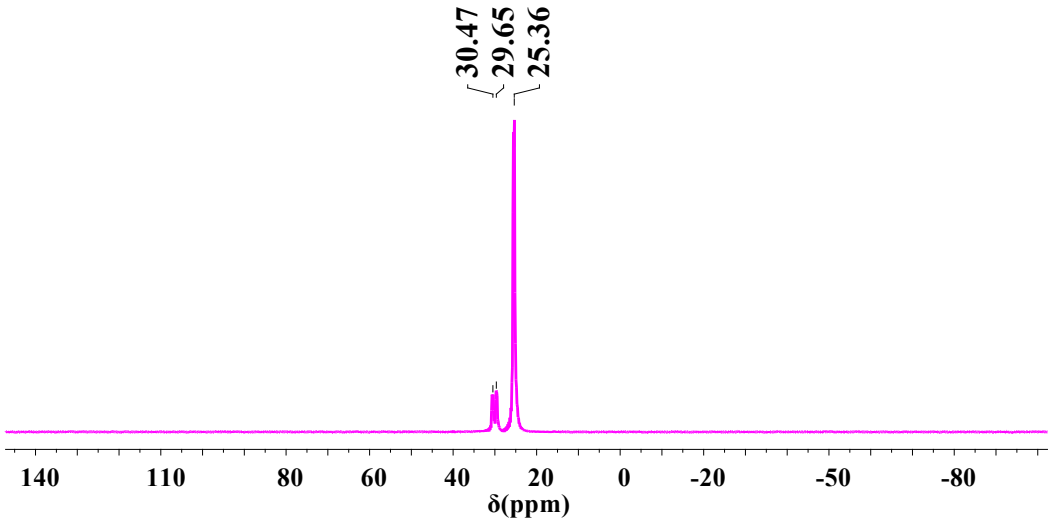

Fig. S4 The CP-MAS ^{13}C NMR spectrum of [(^{t}BuPO$_3$H)Li(H$_2$O)$_3$·(H$_2$O)] **1** (150 MHz).

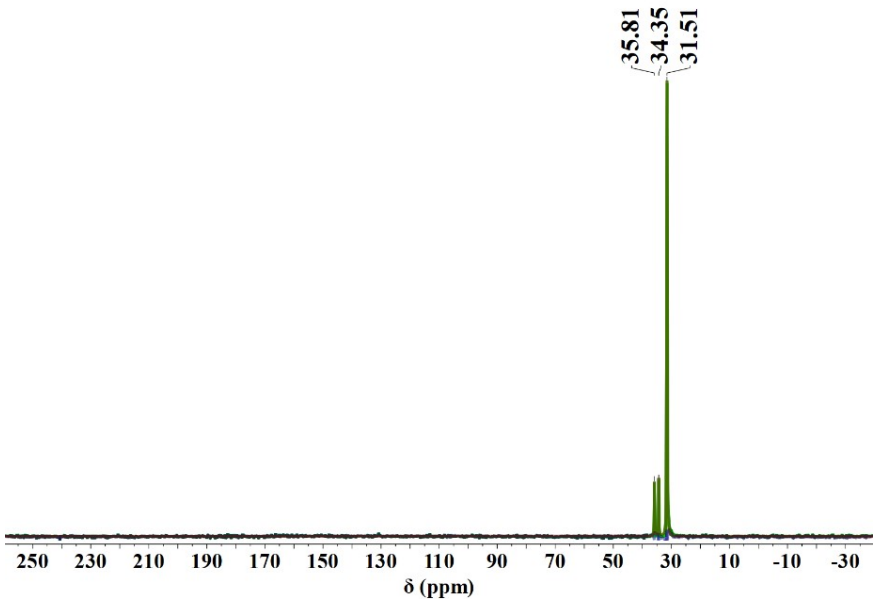

Fig. S5 The CP-MAS ^{13}C NMR spectrum of $[(^{t}BuPO_3)Na_2(H_2O)_4]_n$ **2** (100 MHz).

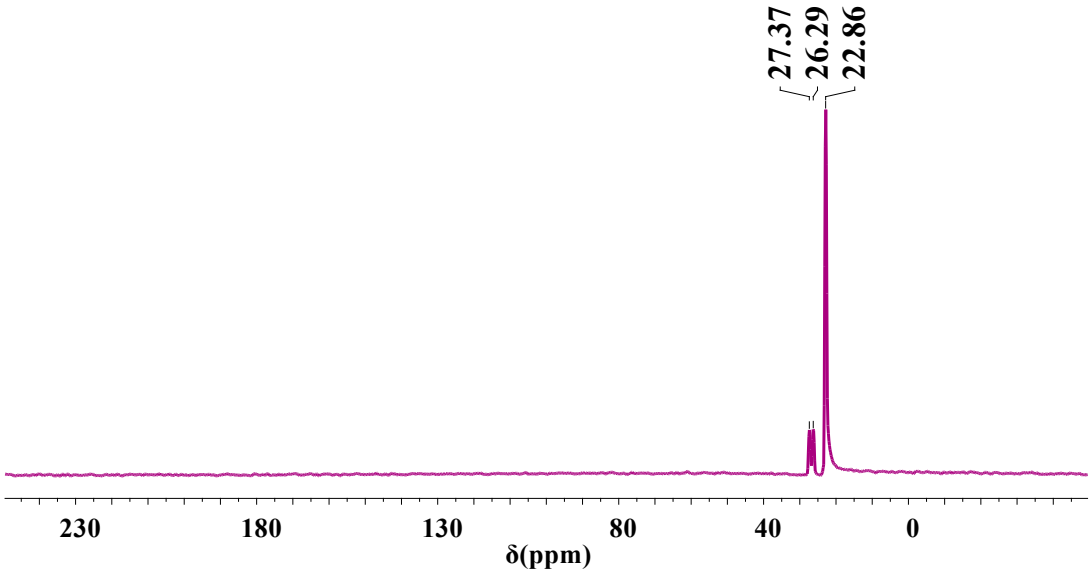

Fig. S6 The CP-MAS ^{13}C NMR spectrum of $[(^{t}BuPO_3H)K(H_2O)]_n$ **3** (125 MHz).

SHAPE analysis of alkali metals centers in 1-3

The coordination environment of the tetra-coordinated Li-ion in complex **1** adopts a tetrahedral shape, while the $Na_1(I)$ exhibits an octahedron environment, and $Na_2(I)$ displays a vacant trigonal bipyramid**.** The geometry of the K(I) in compound **3** takes on a capped trigonal prism configuration. These geometries were analyzed by SHAPE 2.1 software. Continuous Shape measurements reveal that the core geometries of the alkali metal center in all three complexes (**1-**

3) differ, with minimal deviation from ideal ***Td*** symmetry in compound **1**, ***Oh*** and $\boldsymbol{C_{3v}}$ symmetry in compound **2**, and similarly $\boldsymbol{C_{2v}}$ symmetry in compound **3**.

Table S1 Shape analysis in complex **1** (Li atom)

Structure	SP-4	**T-4**	SS-4	vTBPY-4
Shape	Square	**Tetrahedron**	Seesaw	Vacant trigonal bipyramid
Symmetry	D_{4h}	***Td***	C_{2v}	C_{3v}
Deviation	32.344	**0.126**	8.413	2.708

Table S2 Shape analysis in complex **2** (Na_1 atom)

Structure	HP-6	PPY-6	**OC-6**	TPR-6	JPPY-6
Shape	Hexagon	Pentagonal pyramid	**Octahedron**	Trigonal prism	Johnson pentagonal pyramid J2
Symmetry	D_{6h}	C_{5v}	***Oh***	D_{3h}	C_{5v}
Deviation	30.058	27.009	**0.476**	14.939	29.924

Shape analysis in complex **2** (Na_2 atom)

Structure	SP-4	T-4	SS-4	**vTBPY-4**
Shape	Square	Tetrahedron	Seesaw	**Vacant trigonal bipyramid**
Symmetry	D_{4h}	*Td*	C_{2v}	$\boldsymbol{C_{3v}}$
Deviation	25.365	3.982	3.788	**1.660**

Table S3 Shape analysis in complex **3** (K atom)

Structure	HP-7	HPY-7	PBPY-7	COC-7	**CTPR-7**	JPBPY-7	JETPY-7
Shape	Heptagon	Hexagonal pyramid	Pentagonal bipyramid	Capped octahedron	**Capped trigonal prism**	Johnson pentagonal bipyramid J13	Johnson elongated triangular pyramid J7
Symmetry	D_{7h}	C_{6v}	D_{5h}	C_{3v}	$\boldsymbol{C_{2v}}$	D_{5h}	C_{3v}
Deviation	33.211	19.510	8.228	4.176	**3.491**	10.491	18.536

Table S4 Selected bond distances (Å) and bond angles (°) in **1**.

Li(1)–O(1)	1.906(5)	O(1)–Li(1)–O(4)	115.6(3)
Li(1)–O(4)	1.938(5)	O(1)–Li(1)–O(5)	109.7(2)
Li(1)–O(5)	1.975(5)	O(1)–Li(1)–O(6)	111.9(2)
Li(1)–O(6)	1.959(5)	O(4)–Li(1)–O(5)	103.9(2)
P(1)–O(1)	1.503(2)	O(4)–Li(1)–O(6)	109.3(2)
P(1)–O(2)	1.508(2)	O(6)–Li(1)–O(5)	105.7(2)
P(1)–O(3)	1.591(2)		

Table S5 Hydrogen bonds table for **1** [Å and °].

D–H···A	**d(D-H) [Å]**	**d(D-H) [Å]**	**d(D-A) [Å]**	**∠D-H-A [°]**
O(3)–H(3)···O(7)	0.84	1.80	2.585(3)	153.9
O(4)–H(4A)···O(5)$^{\#1}$	0.85	2.03	2.862(3)	165.1
O(5)–H(5A)···O(6)$^{\#2}$	0.85	1.91	2.768(3)	175.9
O(5)–H(5B)··· O(7)	0.80(4)	2.03(4)	2.797(3)	161(3)
O(6)–H(6A)··· O(2)$^{\#3}$	0.85	1.85	2.680(3)	163.5
O(6)–H(6B)··· O(3)$^{\#4}$	0.85	2.01	2.802(3)	154.1
O(7)–H(7A)··· O(1)$^{\#5}$	0.85	1.89	2.730(3)	170.4
O(7)-H(7B)··· O(2) $^{\#3}$	0.82(5)	1.88(5)	2.665(3)	161(4)

Symmetry transformations used to generate equivalent atoms: $^{\#1}$1-X,1-Y,1-Z; $^{\#2}$1-X,2-Y,1-Z; $^{\#3}$+X,1+Y,+Z; $^{\#4}$-1+X,1+Y,+Z; $^{\#5}$1+X,+Y,+Z.

Table S6 Selected bond distances (Å) and bond angles (°) in **2**.

Na(1)–O(4) #1	2.374(4)	O(4)#2–Na(1)–O(7)	94.3(1)
Na(1)–O(4)	2.323(4)	O(4)1–Na(1)–O(7)	83.9(1)
Na(1)–O(5)	2.523(4)	O(5)–Na(1)–O(7)	175.3(1)
Na(1)–O(6) #2	2.325(4)	O(6)–Na(1)–O(4)	99.0(1)
Na(1)–O(6)	2.301(4)	O(6)–Na(1)–O(4)#2	84.6(1)
Na(1)–O(7)	2.558(4)	O(6)#1–Na(1)–O(4)#2	91.1(1)
Na(2)–O(1)	2.807(5)	O(6) #1–Na(1)–O(5)	89.5(1)
Na(2)–O(3) #4	2.676(5)	O(6)–Na(1)–O(5)	92.8(1)
Na(2)–O(4)	2.794(5)	O(6)–Na(1)–O(6)#1	175.1(1)
Na(2)–O(6)#3	2.713(5)	O(6)#1–Na(1)–O(7)	87.3(3)
P(1)–O(1)	1.596(3)	O(6)–Na(1)–O(7)	90.8(1)
P(1)–O(2)	1.502(4)	O(3)#4–Na(2)–O(1)	107.0(2)
P(1)–O(3)	1.514(3)	O(3)#4–Na(2)–O(4)	99.8(2)
O(4)–Na(1)–O(4)#2	176.0(1)	O(3)#4–Na(2)–O(6)#3	115.9(2)
O(4)#2–Na(1)–O(5)	89.1(1)	O(4)–Na(2)–O(1)	95.8(2)
O(4)–Na(1)–O(5)	92.5(1)	O(6)#3–Na(2)–O(1)	137.4(22)
O(4)–Na(1)–O(6)#1	85.2(1)	O(6)#3–Na(2)–O(4)	83.1(1)

Symmetry transformations used to generate equivalent atoms: #1 1-X,-1/2+Y,1/2-Z; #2 1-X,1/2+Y,1/2-Z; #3 1-X,1-Y,1-Z; #4 +X,-1+Y,+Z; #5 +X,1+Y,+Z.

Table S7: Hydrogen bonds (Å) and angles (°) for **2**.

D−H···A	d(D−H)	d(H···A)	d(D···A)	<(DHA)
O(5)−H(5A)···O(7) #1	0.89(2)	1.98(3)	2.856(5)	166(6)
O(5)−H(5B)···O(2) #2	0.68(7)	2.16(7)	2.837(5)	171(8)

Symmetry transformations used to generate equivalent atoms: #1 1-X,-1/2+Y,1/2-Z; #2 +X,3/2-Y,-1/2+Z.

Table S8 Selected bond distances (Å) and bond angles (°) in **3**.

K(1)–O(1)#1	2.835(4)	O(1)#1–K(1)–O(4)#4	89.0(1)
K(1)–O(1)	2.712(4)	O(1)#1–K(1)–O(4)#5	155.7(1)
K(1)–O(3)#3	2.742(4)	O(1)–K(1)–O(4)	53.0(1)
K(1)–O(3)#1	2.944(4)	O(1)–K(1)–O(4)#5	74.9(1)
K(1)–O(4)#4	2.836(4)	O(3)#3–K(1)–O(1)#1	118.7(1)
K(1)–O(4)	3.306(4)	O(3)#3–K(1)–O(3)#1	77.8(8)
K(1)–O(4)#5	2.857(4)	O(3)#3–K(1)–O(4)#5	85.4(1)
P(1)–O(1)	1.503(4)	O(3)#1–K(1)–O(4)	74.6(1)

P(1)–O(2)	1.577(4)	O(3)$^{\#3}$–K(1)–O(4)	96.5(1)
P(1)–O(3)	1.508(4)	O(3)$^{\#3}$–K(1)–O(4)$^{\#4}$	99.5(1)
O(1)–K(1)–O(1)$^{\#1}$	84.7(1)	O(4)$^{\#4}$–K(1)–O(3)$^{\#1}$	127.8(1)
O(1)–K(1)–O(3)$^{\#3}$	146.1(1)	O(4)$^{\#5}$–K(1)–O(3)$^{\#1}$	145.8(1)
O(1)$^{\#1}$–K(1)–O(3)$^{\#1}$	51.8(1)	O(4)$^{\#5}$–K(1)–O(4)	78.0(9)
O(1)–K(1)–O(3)$^{\#1}$	103.5(1)	O(4)$^{\#4}$–K(1)–O(4)$^{\#5}$	83.9(1)
O(1)$^{\#1}$–K(1)–O(4)	100.3(1)	O(4)$^{\#4}$–K(1)–O(4)	154.8(7)
O(1)–K(1)–O(4)$^{\#4}$	105.5(1)		

Symmetry transformations used to generate equivalent atoms: $^{\#1}$1-X,1-Y,1-Z; $^{\#2}$1-X,1-Y,2-Z; $^{\#3}$1-X,1/2+Y,3/2-Z; $^{\#4}$1-X,-1/2+Y,3/2-Z; $^{\#5}$+X,3/2-Y,1/2+Z.

Table S9 Hydrogen bonds (Å) and angles (º) for **3.**

D–H···A	d(D–H)	d(H···A)	d(D···A)	<(DHA)
O(2)–H(2)···O(3)$^{\#1}$	0.84	1.77	2.568(5)	157.9

Symmetry transformations used to generate equivalent atoms: $^{\#1}$+X,1/2-Y,1/2+Z.

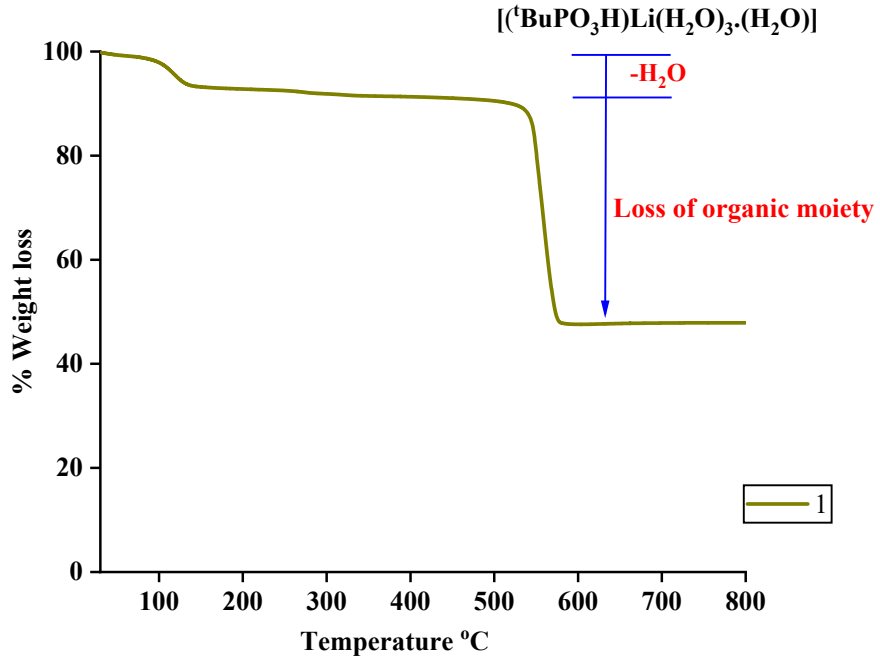

Fig. S7 TGA profile of **1** recorded under a flow of N_2 at a heating rate of 10 °C min^{-1}.

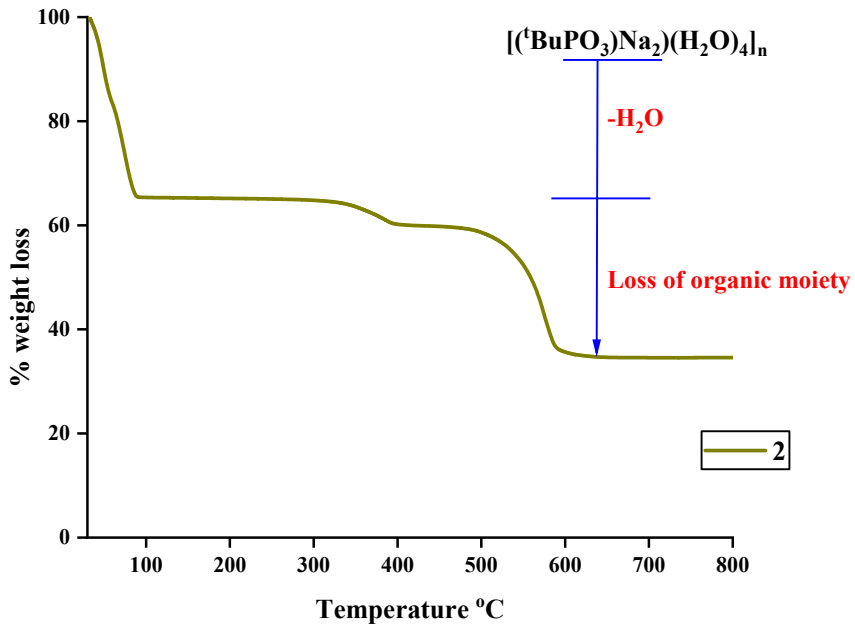

Fig. S8 TGA profile of **2** recorded under a flow of N_2 at a heating rate of 10 °C min^{-1}.

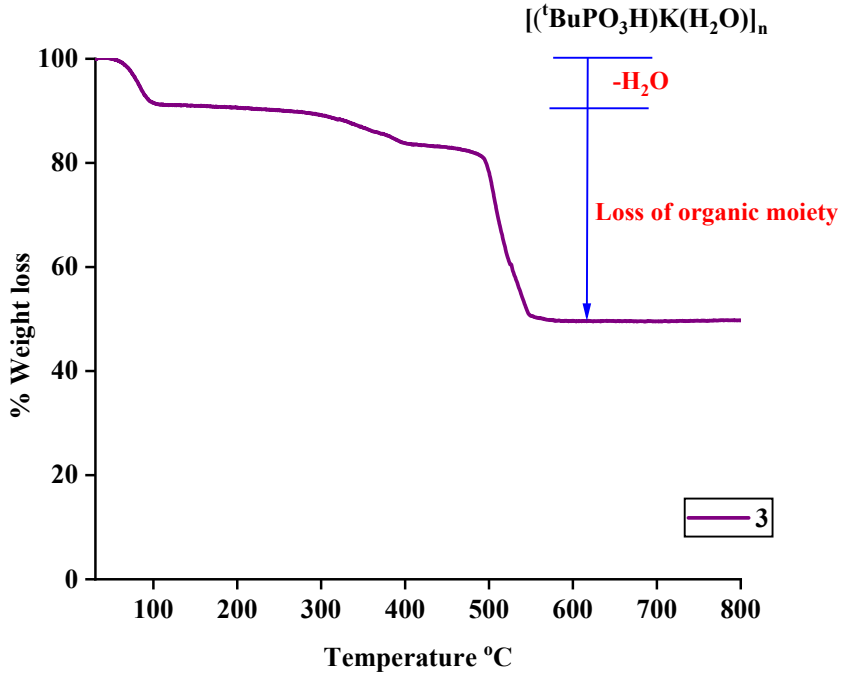

Fig. S9 TGA profile of **3** recorded under a flow of N_2 at a heating rate of 10 °C min^{-1}.

SEM morphological studies of alkali metals tert-butyl phosphonates 1-3

The morphological features of alkali metal tert-butyl phosphonate compounds **1**, **2**, and **3** were investigated by a field emission scanning electron microscope (FEG_SEM). The FEG-SEM images revealed a layered sheet kind of morphology of compounds **1**, **2**, in (Fig. S10 and S11) and **3** was shown (Fig. S12), which has been further corroborated by the single-crystal X-ray diffraction experiments (vide supra). Comparing the surface roughness of compounds **2** and **3** exhibited a higher degree of roughness compared to compound **1**. The average size of the synthesized sheet-like structures ranged from a few micro to 15 μm. Notably, the compound **3** exhibited a unique feature where the single sheet rolled up to form a tubular structure reminiscent of carbon nanotubes (Fig. S13) Furthermore, SEM-EDX mapping confirmed the uniform distribution of the respective elements throughout the layered sheet structure of compounds **1**, **2**, and **3**, indicating the consistent composition and structure of these materials.

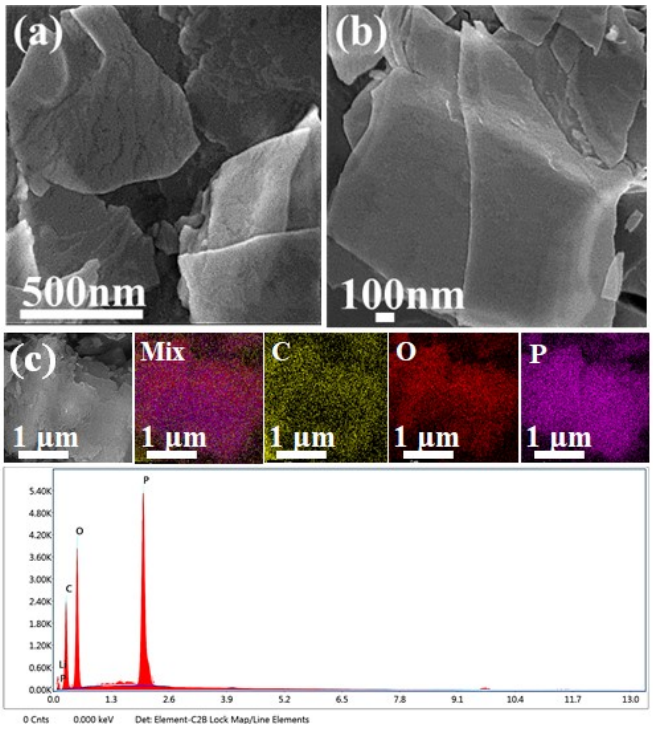

Fig. S10 SEM images of compound **1**, (a) and (b) showing layered structures; (c) EDX spectrum of **1** with elemental mapping.

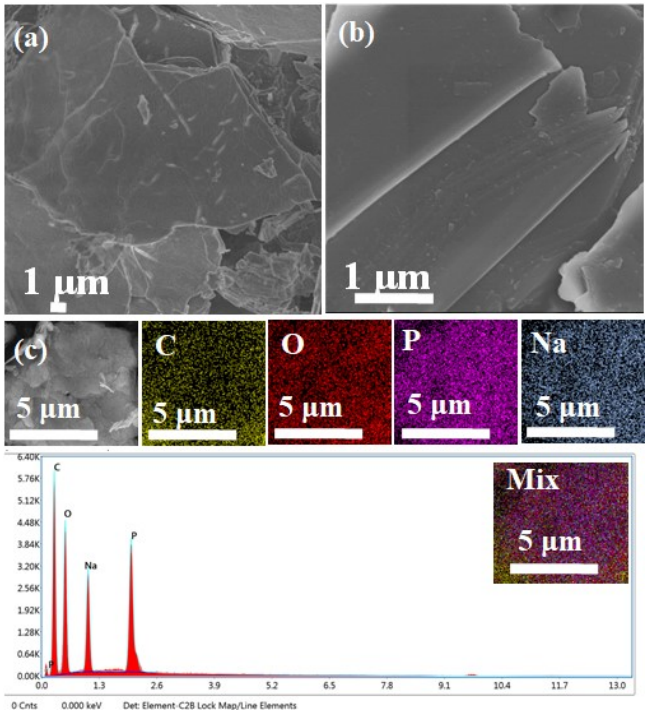

Fig. S11 SEM images of compound **2** (a) and (b) showing layered structures; (c) EDX spectrum of **2** with elemental mapping.

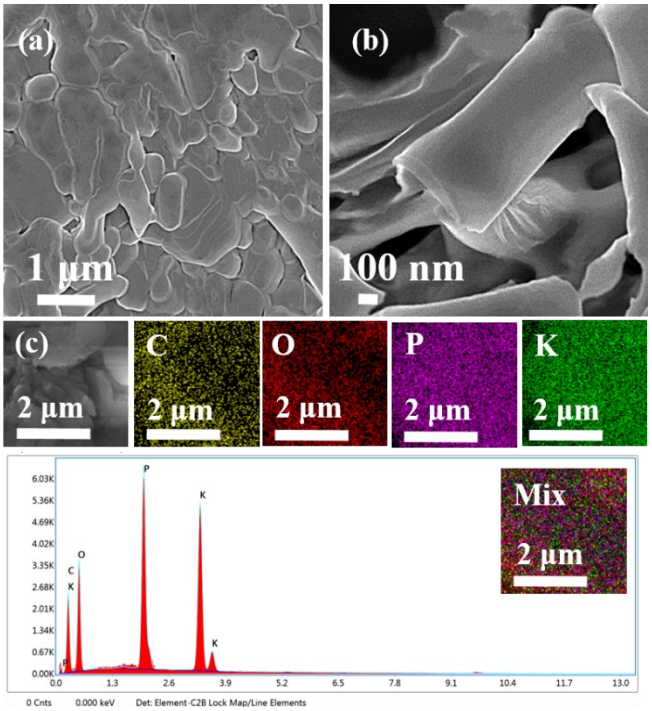

Fig. S12 SEM images of compound **3**; (a) and (b) showing layered structures; (c) EDX spectrum of **3** with elemental mapping.

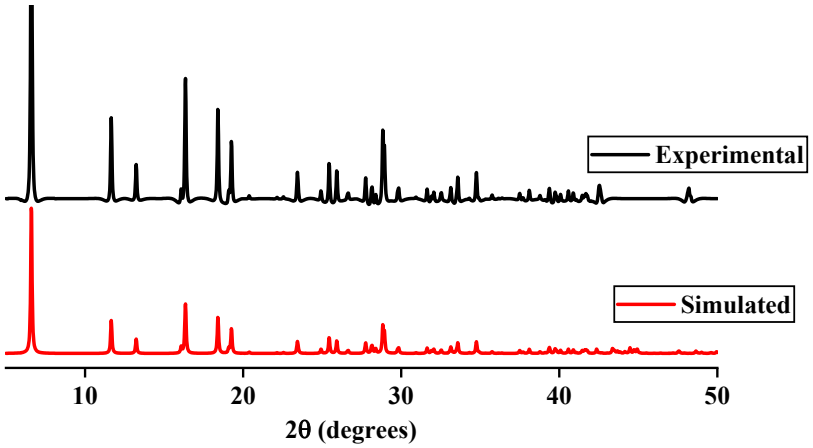

Fig. S13 PXRD pattern of **1**

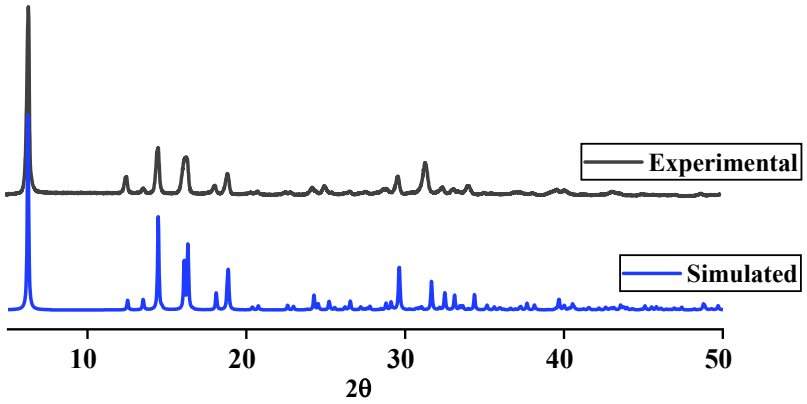

Fig. S14 PXRD pattern of **2**

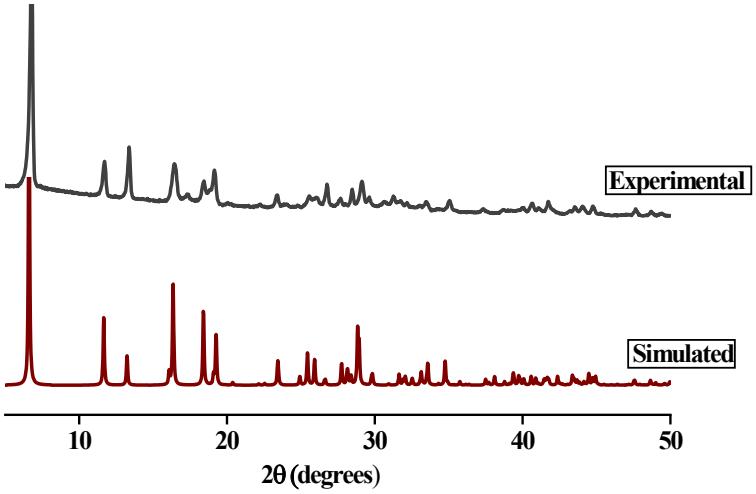

Fig. S15 PXRD pattern of **3**

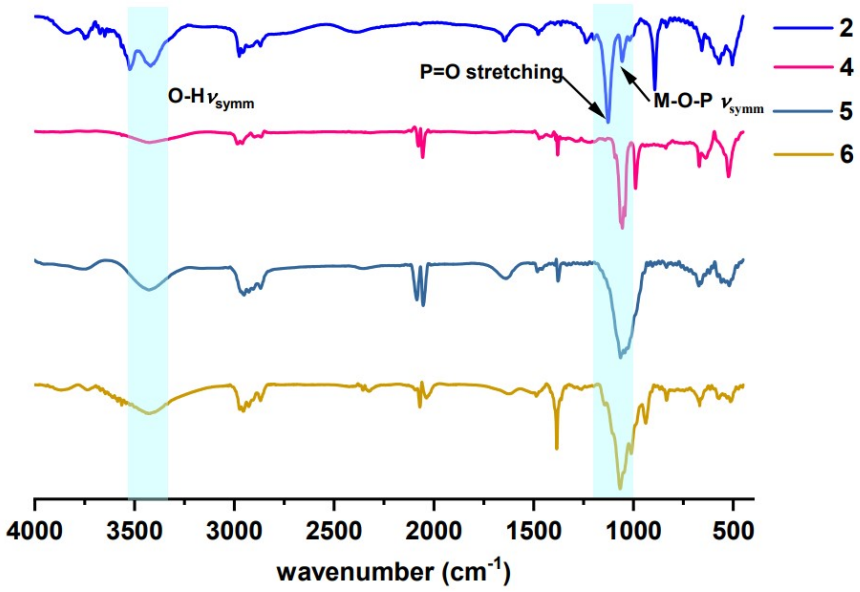

Fig. S16 Comparison of FT-IR spectra of **4-6** with **2** (as KBr diluted disc).

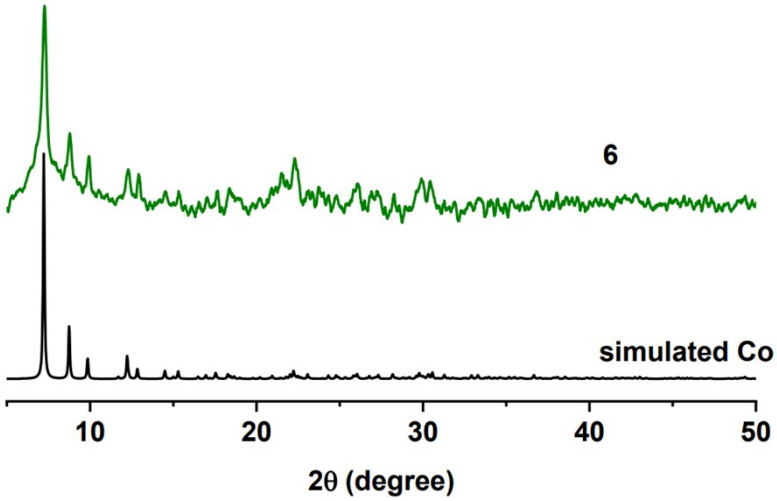

Fig. S17 PXRD pattern of $[(^{t}BuPO_3)Co(H_2O)]_n$ **6**.

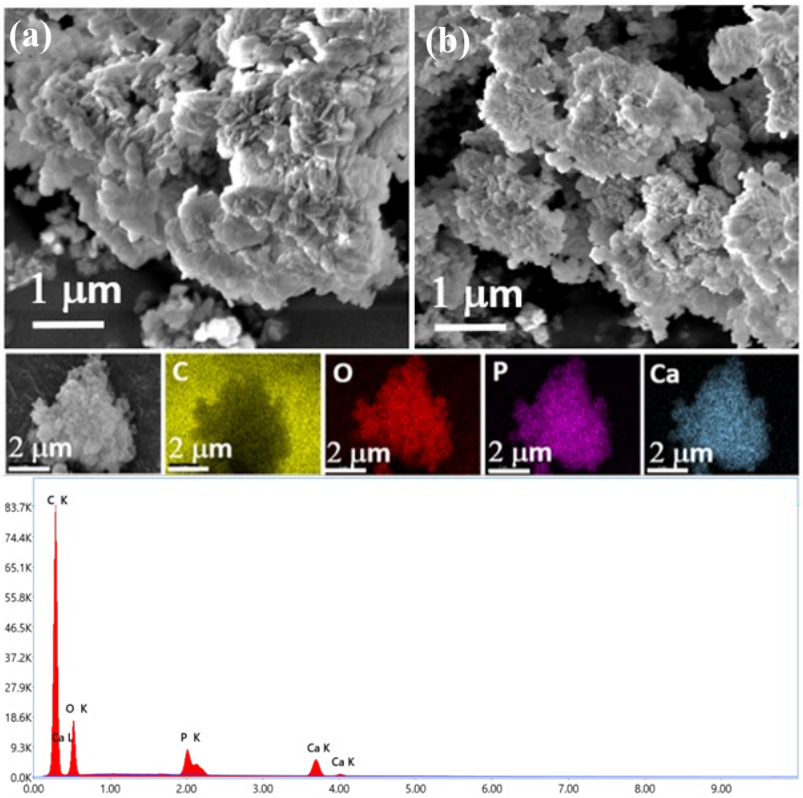

Fig. S18 SEM images of compound **4**; (a) and (b) showing layered structures; (c) EDX spectrum of **6** with elemental mapping. (compound was SEM beam sensitive)

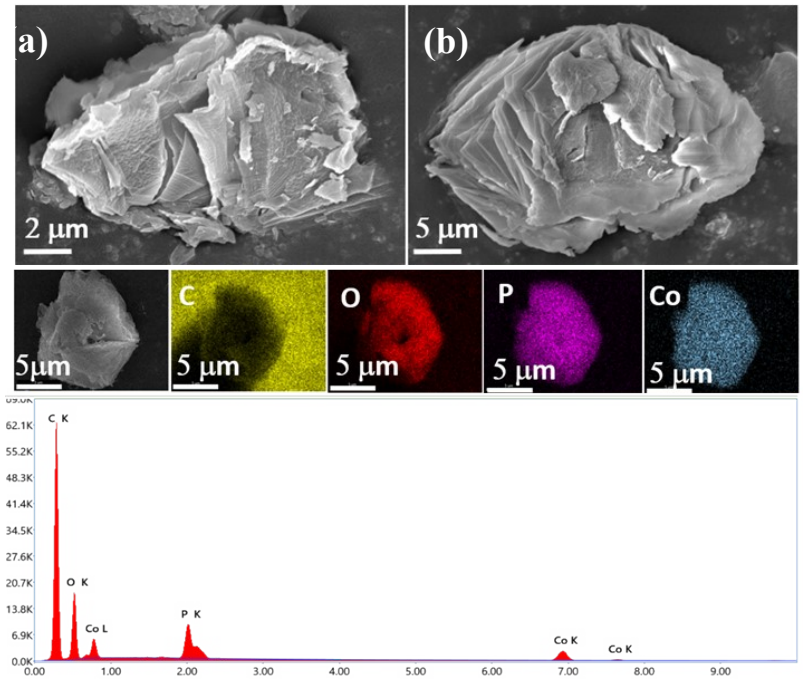

Fig. S19 SEM images of compound **6**; (a) and (b) showing layered structures; (c) EDX spectrum of **6** with elemental mapping.

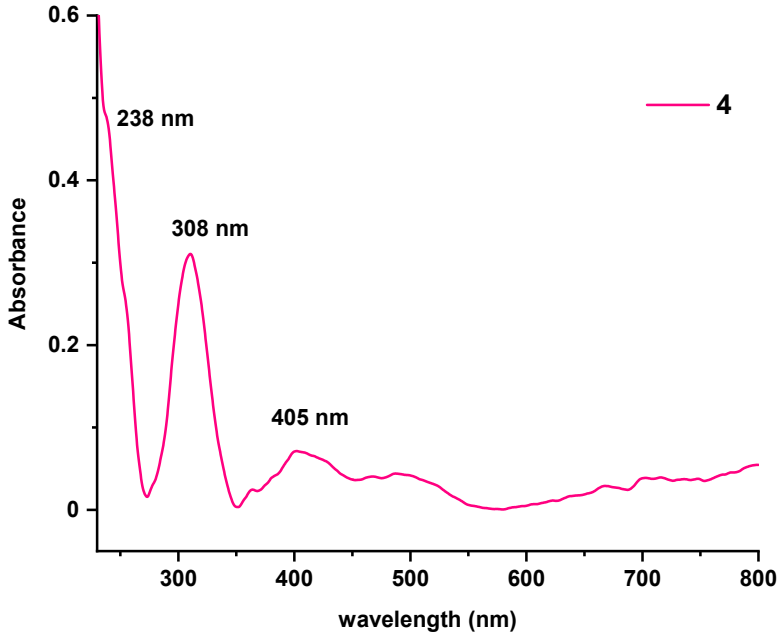

Fig. S20 DR-UV of $[(^{t}BuPO_3)Ca(H_2O)]_n$ (**4**).

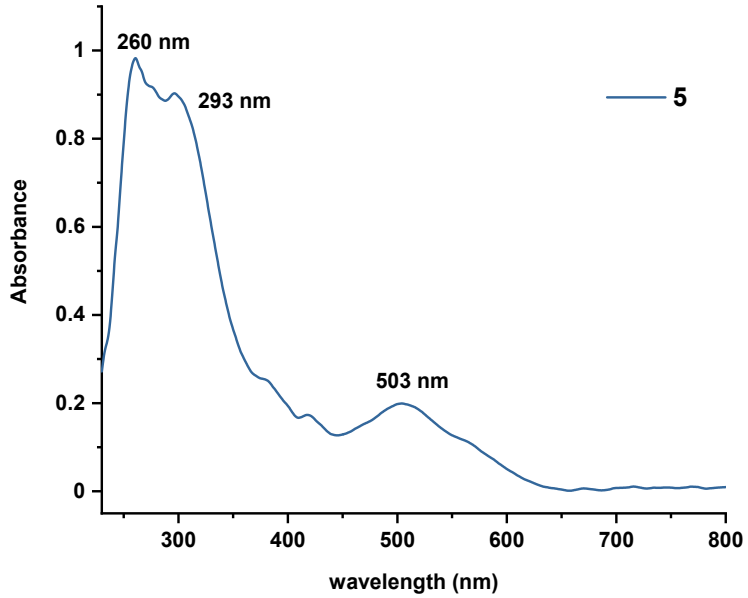

Fig. S21 DR-UV of $[(^{t}BuPO_3)Mn(H_2O)]_n$ (**5**).

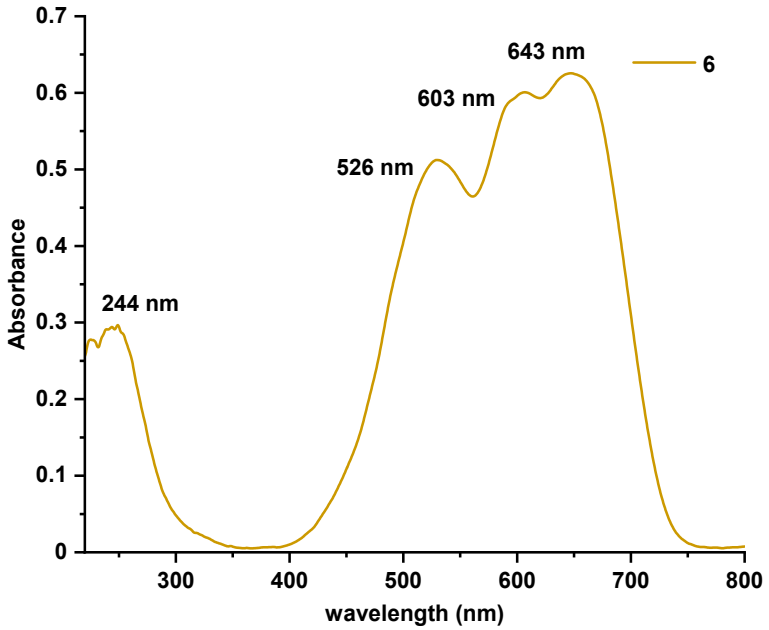

Fig. S22 DR-UV of $[(^{t}BuPO_3)Co(H_2O)]_n$ (**6**).

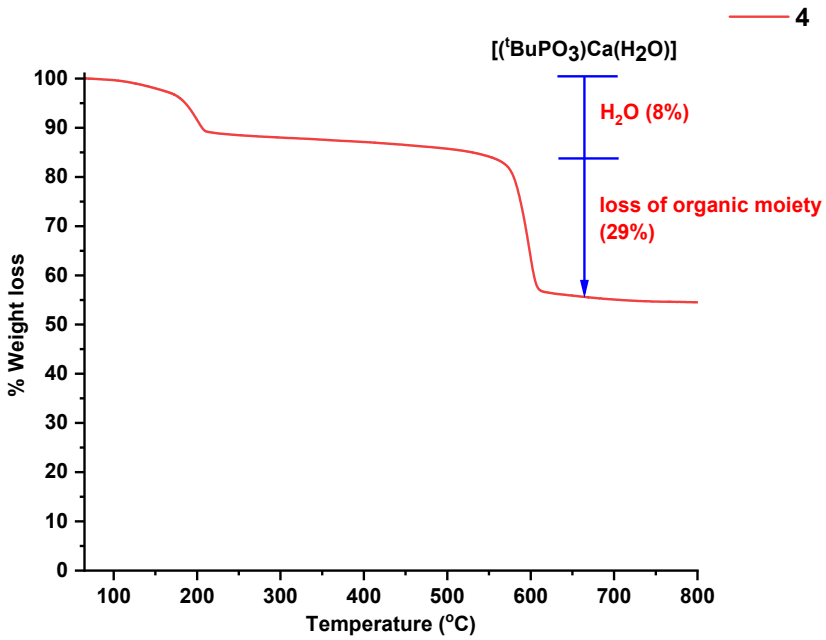

Fig. S23 TGA profile of compound **4** recorded under a flow of N_2 at a heating rate of 10 °C min^{-1}.

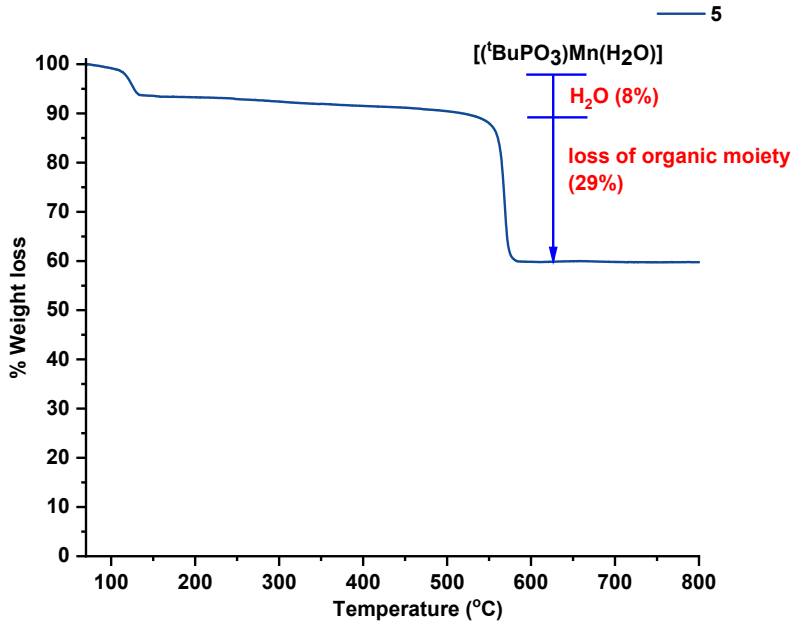

Fig. S24 TGA profile of compound **5** recorded under a flow of N_2 at a heating rate of 10 °C min^{-1}.

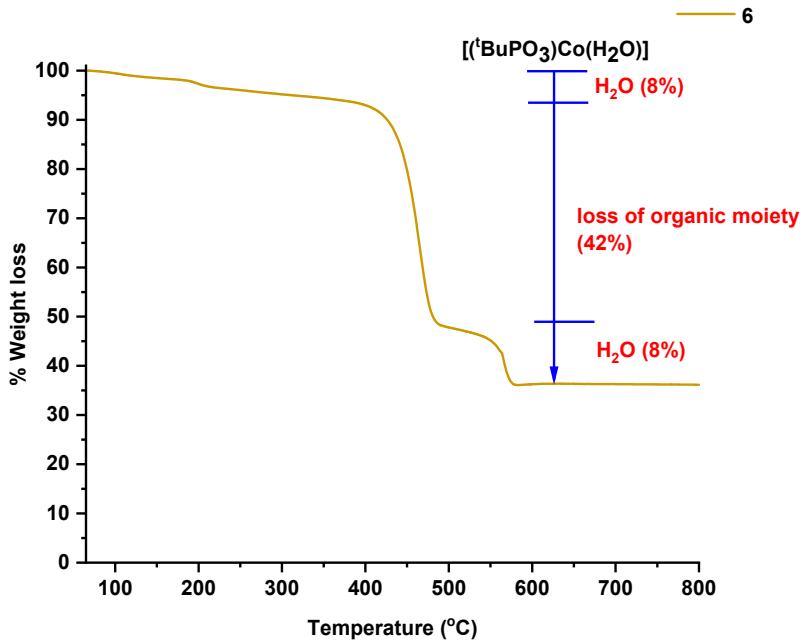

Fig. S25 TGA profile of compound **6** recorded under a flow of N_2 at a heating rate of 10 °C min^{-1}.

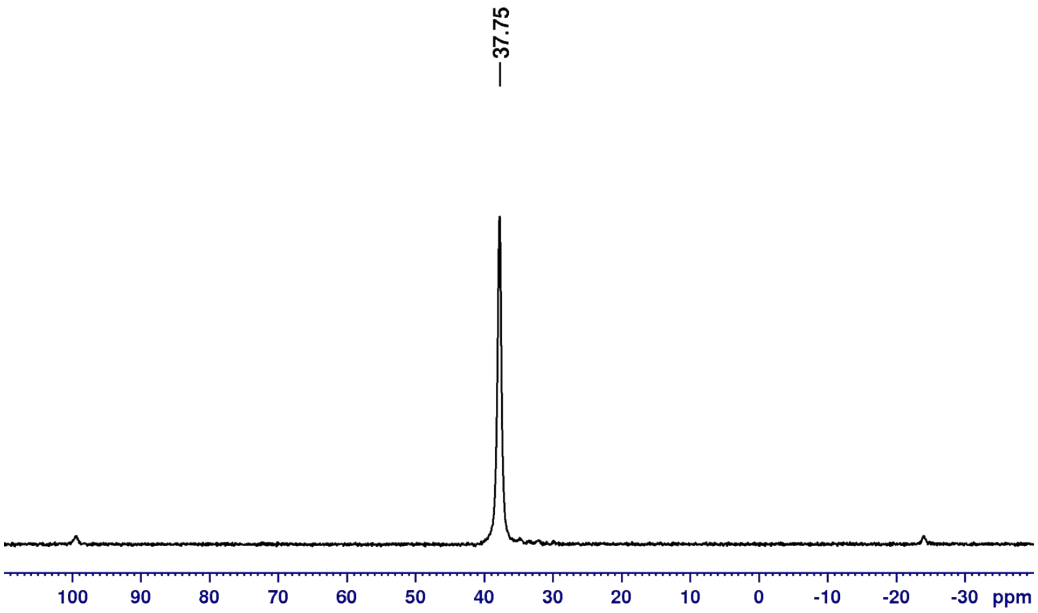

Fig. S26 CP-MAS ^{31}P NMR spectrum of [(^{t}BuPO$_3$)Ca(H$_2$O)]$_n$ **4** (162 MHz).

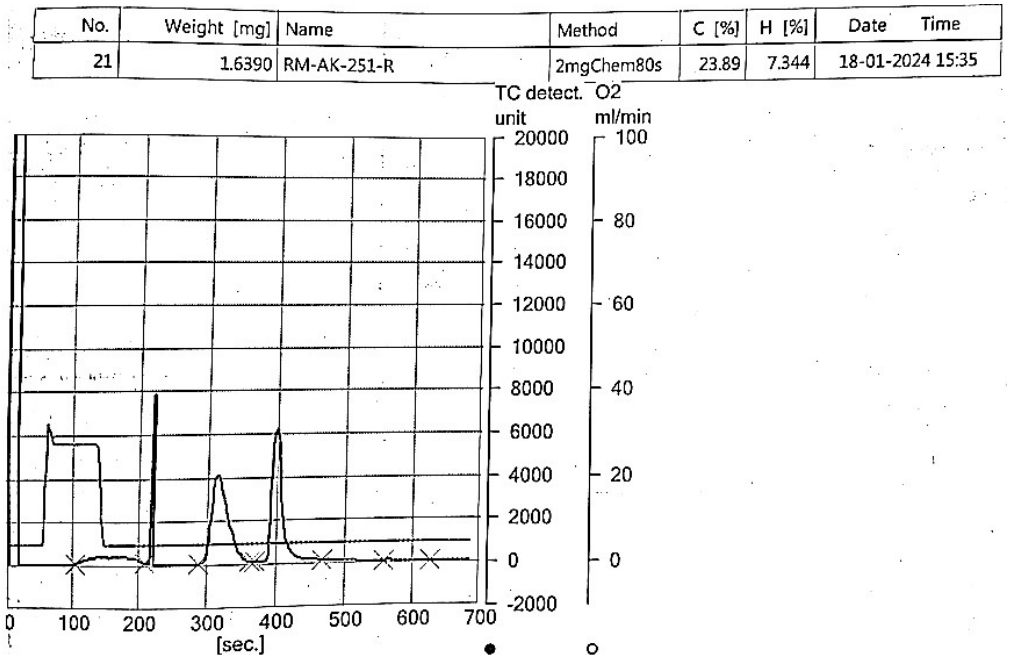

Fig. S27 Elemental analysis of [^{t}BuPO$_3$HLi(H$_2$O)$_3$·(H$_2$O)] (**1**).

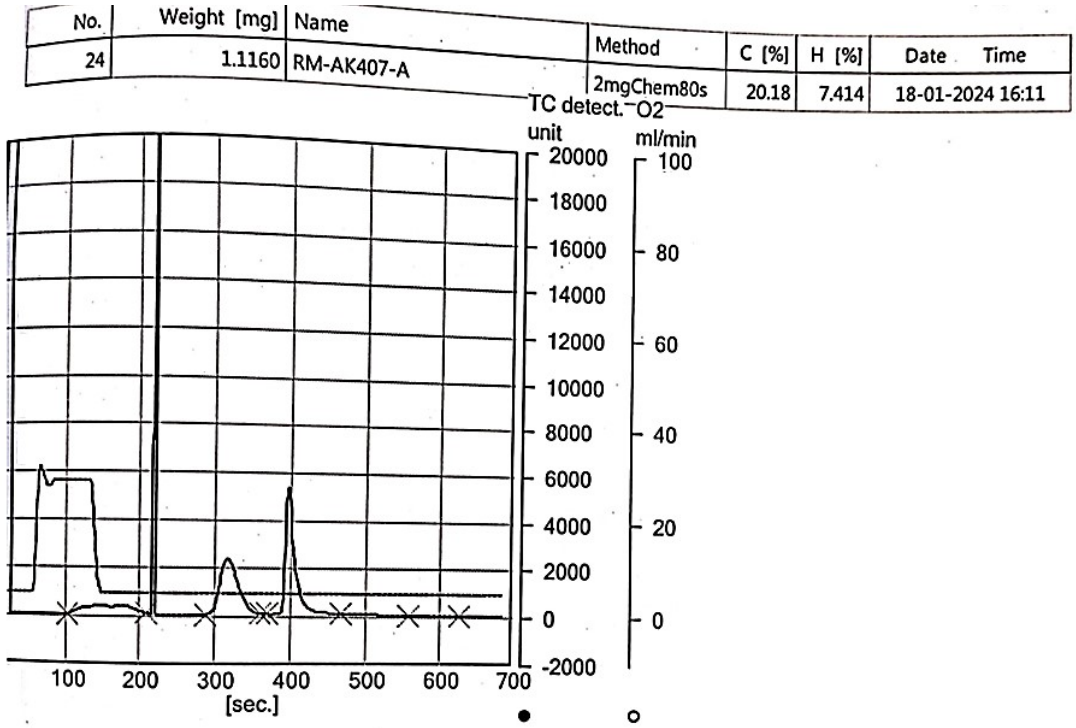

Fig. S28 Elemental analysis of $[(^{t}BuPO_3Na_2)(H_2O)_4]_n$ (**2**).

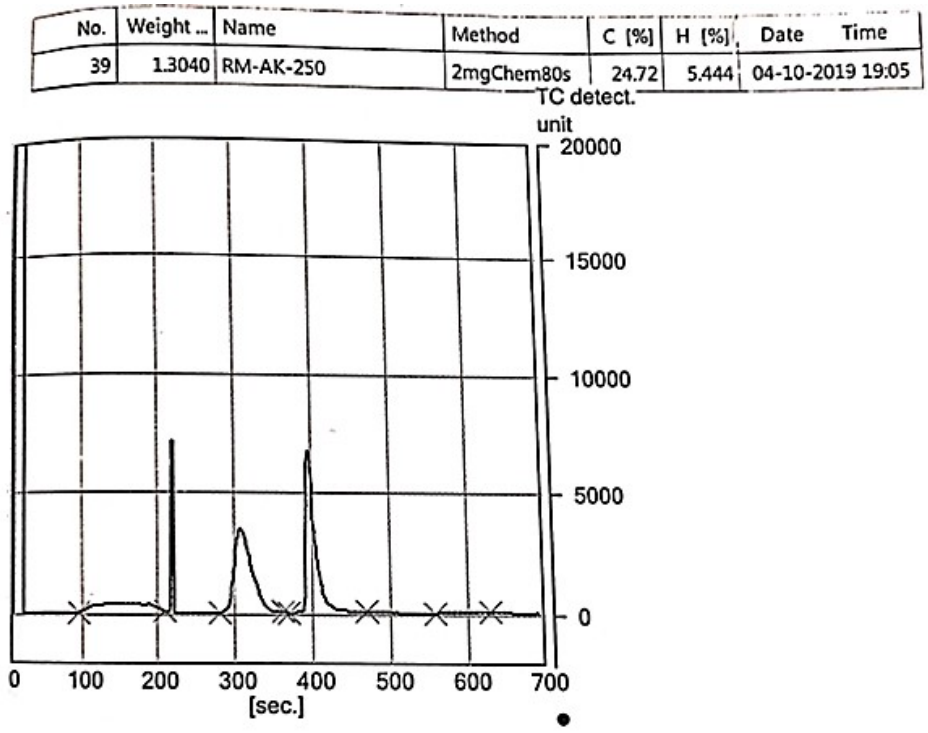

Fig. S29 Elemental analysis of $[^{t}BuPO_3HK(H_2O)]_n$ (**3**).

No.	Weight [mg]	Name	Method	N [%]	C [%]	H [%]	Date Time
21	1.3150	RM-AG-Ca	2mgChem80s	0.00	25.23	5.553	04-04-2024 15:06

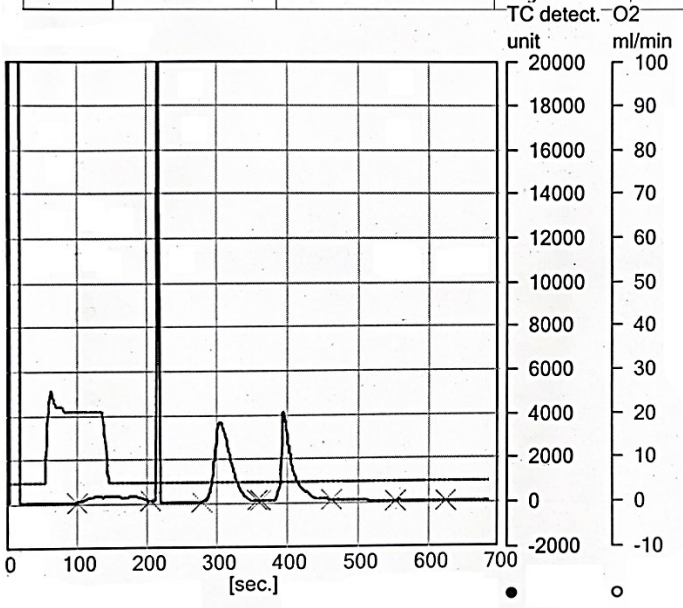

Fig. S30 Elemental analysis of $[^{t}BuPO_3Ca(H_2O)]_n$ (**4**).

No.	Weight [mg]	Name	Method	N [%]	C [%]	H [%]	Date Time
29	1.5850	RM-AG-Mn	2mgChem80s	0.00	22.96	5.272	04-04-2024 16:40

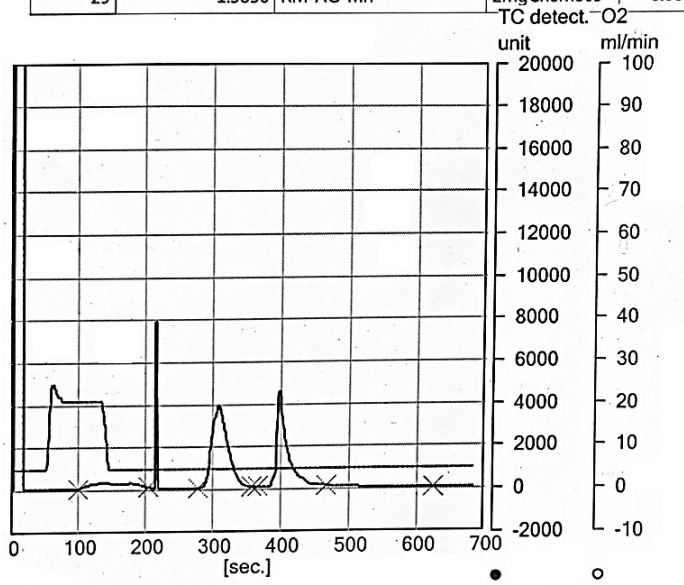

Fig. S31 Elemental analysis of $[^{t}BuPO_3Mn(H_2O)]_n$ **(5)**.

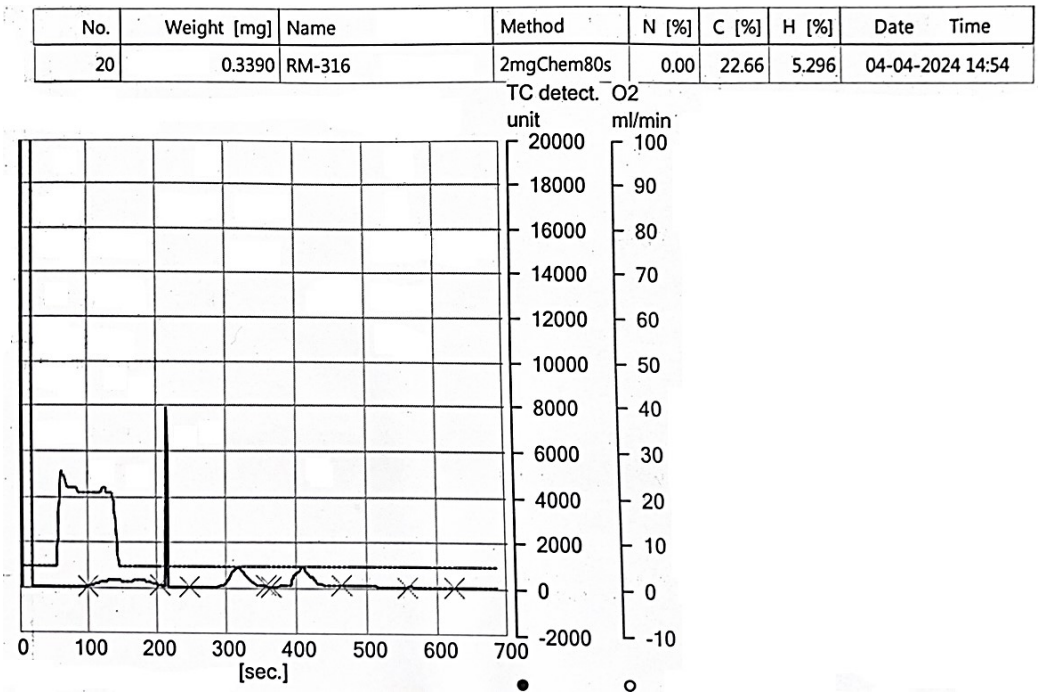

Fig. S32 Elemental analysis of [^{t}BuPO$_3$Co(H$_2$O)]$_n$ (**6**).

Table S10. Chemical composition of **1**-**3** measured with ICP-AES

Sample code	Metal (M)	Metal (ppm)	M (%)	P (ppm)	P (%)	n(M)/n(P)
1	Li	3.826	0.55	14.271	0.46	1.19
2	Na	10.235	0.44	12.809	0.41	1.07
3	K	35.806	0.91	25.281	0.81	1.12

Table S11. Chemical composition of **4**-**6** measured with ICP-AES

Sample code	Metal (M)	Metal (ppm)	M (%)	P (ppm)	P (%)	n(M)/n(P)
4	Ca	18.481	0.46	11.74	0.38	1.21
5	Mn	25.764	0.46	11.176	0.36	1.27
6	Co	24.694	0.41	12.549	0.41	1